IUST
Iran University of Science and Technology

Iranian Journal of Electrical and Electronic Engineering

Journal Homepage: ijeee.iust.ac.ir

Performance Comparison of Hybrid Switch, Phase Shifter and Lens Network over Hybrid Beamforming in Millimeter Wave Massive MIMO

Tadele A. Abose*(C.A.), Thomas O. Olwal**, Abel D. Daniel*** and Murad R. Hassen****

Abstract: Due to cost and energy concerns with digital beamformers, much of the beamforming is done by hybrid beamformers in mm-wave (mm) massive multiple input multiple output (MIMO). Various works in hybrid beamforming structures considered either phase shifters, switches, or radio frequency lenses individually as switching mechanisms between antennas and precoding systems. Works that consider the hybrid use of phase shifters, switches, and radio frequency lenses need further investigation since there is a tradeoff between cost and system performance in each switching mechanism. The main aim of this research is to analyze the performance of a hybrid switch, a 1-bit phase shifter, and radio frequency (RF)-Lens in a hybrid beamforming network as a switching network. Simulation results showed that the hybrid of three has a spectral efficiency (SE) performance of 59.04 bps/Hz, which increases by 6.9 bps/Hz from that of the switch and lens antenna array network. The energy efficiency (EE) of the switch, phase shifter, and lens showed a performance of 46.41 bps/Hz/W, while the switch and lens antenna array, phase shifter, and lens antenna array showed a performance of 48.52 bps/Hz/W. The result also shows that the hybrid network achieves optimum performance at the expense of higher computational complexity.

Keywords: 1-bit Phase Shifter, Hybrid Beamforming, Lens Antenna Array, Multiple Input Multiple Output, Radio Frequency Chain, Switch.

1 Introduction

IN comparison to conventional multiple input multiple output (MIMO) systems, massive MIMO systems offer higher quality of service (QoS) and spectral efficiency by combining hundreds of antennas to serve dozens of user equipment (UEs) simultaneously. Customers requiring higher-bandwidth technologies will need an infrastructure that is significantly denser in order to meet their demands, as the need for high-speed data rates and network connectivity continues to rise. Massive MIMO combined with millimeter waves (mm) results in high spectral efficiency and a significant boost in data throughput. Another strategy under investigation to reduce interference and boost overall capacity is spatial directivity. In order to take advantage of spatial degrees of freedom, MIMO wireless technology uses multiple antennas on both the transmit and receive sides (or multiple antenna beams in a wide array scenario). These spatial degrees of freedom are used in single-user systems to both increase the maximum attainable rate and reduce the likelihood of an outage. Cellular service providers are facing unprecedented global spectrum and bandwidth scarcity challenges as a result of the rapidly growing mobile data and consumer base [1].

Thankfully, there is considerable unoccupied spectrum in the mm-wave band, which is the 30–300 GHz frequency range. This spectrum can offer gigahertz

Iranian Journal of Electrical & Electronic Engineering, 2024.
Paper first received 19 March 2024 and accepted 27 June 2024.
* The author is with the Department of Electrical and Computer Engineering, Mattu University, Mattu, Ethiopia.
E-mail: tadele.abera@meu.edu.et
** The author is with the Department of Electrical Engineering/F'SATI, Tshwane University of Technology University, Pretoria, South Africa.
*** The author is with the Department of Electrical and Computer Engineering, Dire Dawa University, Dire Dawa, Ethiopia.
**** The author is with the Department of Electrical and Computer Engineering, Addis Ababa University, Addis Ababa, Ethiopia.
Corresponding Author: Second B. Author.

bandwidth and tens of gigabits per second of data transmission rate, which can significantly increase transmission scale and enhance service quality. However, the propagation condition is unfavorable for mm transmission due to considerable propagation loss, which makes the widespread deployment of wireless millimeter-wave communications technically challenging. It is reasonable to be concerned about the behavior of propagation at mm frequencies, which include greater attenuation of rainfall, air absorbance, and foliage-causing loss. They pose the biggest challenges for mm-wave carriers in long-range communications [2]. However, for mm-wave frequencies, especially at 28 and 38 GHz, rain attenuation and air absorption do not result in a significant path loss when small cells in the urban area (on the scale of 200 m) are considered [3]. Therefore, attenuation can be reduced by utilizing high-density and small-cell base stations. Owing to the limited coverage of the base station, this tactic can cause additional interference for UE in the vicinity. A large-scale antenna array with high array gain should create a highly directed beam to reduce interference, mitigate loss of the path, and increase communication coverage in order to avoid such situations [4]. These features of mm-wave massive MIMO allow for two explanations of how to fully utilize the benefits of mm-wave massive MIMO using beamforming techniques: digital beamforming and analog beamforming. The former is a very practical option. Each antenna element at the base station (BS) and UE in digital beamforming (DB) has its own radio frequency (RF) chain, which consists of an analog to digital converter (ADC), a down-converter, a low-noise amplifier, and so on [5], [6].

Dedicated RF chains for each antenna are inefficient when there is a significant number of base station (BS) antennas due to the high cost and power consumption of mixed signal components like high-resolution ADCs and digital-to-analog converters (DACs) [7]. Consequently, beamforming using fewer RF chains has gained significant attention. Hybrid beamforming (HB), which utilizes beamforming in both digital and analog domains, is one approach to address this challenge. In the analog domain, beamforming is achieved at the radio frequency using cost-effective phase shifters (PSs), while in the digital domain, it is performed at the baseband frequency [8], [9], [10]. The various implementation aspects of HB architecture are thoroughly covered in several studies [11], [12]. In mm-wave MIMO systems, hundreds of antenna elements can be used to provide the array gain necessary to compensate for propagation losses at mm-wave frequencies. However, this benefit comes with increased interference due to the dense arrangement of antennas. Beamforming is employed to mitigate this interference, akin to a traffic signaling system, where RF elements in an antenna array are combined to constructively interfere with transmissions at certain angles while destructively interfering with others [13]. Numerous studies have proposed methods to enhance signal directivity, including the use of antenna arrays and phase shifters.

Switch-based hybrid beamforming is particularly promising for massive MIMO communications in mmWave bands, especially for large-scale antenna arrays [14]. This method simplifies the joint optimization of analog and digital beamformers, reducing hardware complexity. Studies have shown that switch-based hybrid architectures, including heuristic-inspired precoding and networks of switches instead of phase shifters, can reduce signal processing complexity and RF chain costs without significant performance degradation [15]. Combining switches and phase shifters for beamforming over frequency-selective channels balances performance with hardware complexity [16]. These strategies collectively enhance mmWave MIMO systems, offering efficient alternatives to traditional phase shifter-based systems. Numerical examples demonstrate that these techniques can achieve comparable or superior performance with simpler and more cost-effective hardware configurations, underscoring the potential of hybrid beamforming in future mmWave massive MIMO deployments [17], [18].

Different switching techniques, such as phase shifters, switches, and lenses, have been utilized in hybrid beamforming. Combinations of switches, phase shifters, uniform planar arrays (UPAs), and lens-array antennas (LAAs) can be employed, but they must be used carefully due to varying costs and performance impacts. More research is needed on hybrid structures involving phase shifters, switches, and RF lenses, as phase shifter-only networks are expensive and switch-only networks suffer from high insertion loss.

The general objective of this work is to analyze and investigate the performance of a hybrid switch, phase shifter, and RF lens (passive phase shifter) network as compared to switch-only and phase shifter-only hybrid beamforming in mm-wave massive MIMO.

The following is a summary of this paper's significant contributions: 1) By taking into account the hybrid switch, phase shifter, and RF lens (passive phase shifter) networks, we have analyzed and compared the spectral and energy efficiency performance and system complexity of hybrid precoding schemes with the existing state-of-the-art techniques. (2) Examining how the energy, spectral efficiency, and system complexity of hybrid beamforming structures are affected by the hybrid switch, phase shifter, and RF lens (passive phase shifter) network when different channel estimation

techniques are employed, which is important for mm wave systems.

This is how the rest of the paper is organized. While system models and descriptions are presented in Section II, results and discussions are presented in Section III. Section IV concludes the research.

2 System Model

The design and analysis of the overall system will be described using the following system model diagrams: From data transmission to result measurement metrics, a specific channel model and channel estimation algorithm will be selected for the given requirements. Results will be shown using spectral efficiency and energy efficiency metrics.

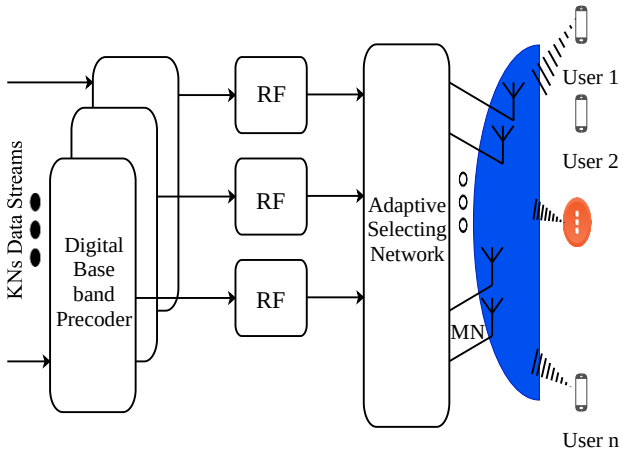

Fig. 1 Overall system design procedure.

The adaptive selecting network can be replaced by the fully or partially connected structures as shown below:

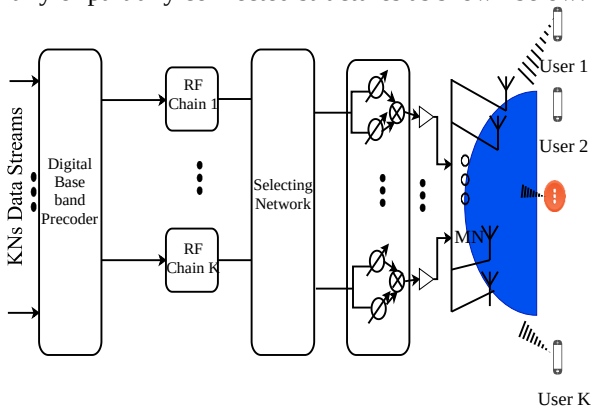

Fig. 2 Partially connected network requiring NM phase shifters and K switching network.

2.1 System Model Explanation

In this research, the energy and spectral efficiency of the hybrid switch, phase shifter, and RF lens network are analyzed for the RF precoder. The system works on a mm-wave based massive MIMO network consisting of a transmit base station equipped with UPA antenna arrays with RF and baseband precoders serving K users using NM antennas. N is the number of transmitting antennas, while M is the number of receiving antennas. The work starts with adopting a channel model and an effective channel estimation technique. The proposed analog network with switch, 1-bit phase shifter, and RF-Lens is designed to create an effective channel matrix using RF, a baseband precoder, and combiners that will give us the new effective downlink vector.

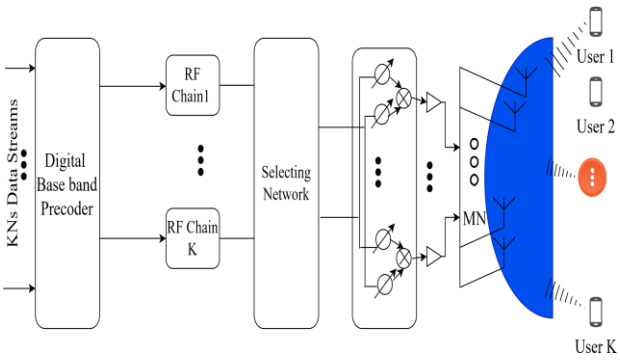

Fig. 3 Fully-connected N^2M 1-bit phase shifter network and K switching network.

Switches are directly connected to the 1-bit phase shifter elements to select antennas with active signals, using a smaller number of RF chains that support the number of users. Fig. 3 shows a fully connected structure where numerous phase shifters are required, but only half as many switches are needed compared to the number of antenna elements, saving on the number of switches. Switches manage an active, fully or partially connected phase shifter network with the respective RF chains, so that not every phase shifter network needs to be connected to the RF chains directly, thereby reducing the number of RF chains to match the number of users. The number of switches is half the number of phase shifters due to each switch's capability to handle connections for several phase shifters, thus reducing the overall number required. This effective design conserves switches while guaranteeing efficient antenna selection and signal routing with a decreased number of RF chains.

2.2 Channel Model

For mm-wave, we employ the widely-used Saleh-Valenzuela channel model. One way to describe the channel matrix is as [19]

$$H = \sqrt{\frac{MN}{P+1}} \sum_{i=0}^{P} \alpha^{(i)} A\left(\xi^{azi(i)}, \xi^{ele(i)}\right) \quad (1)$$

where H $\in R^{MN}$ denotes beamspace channel matrix, P +1 is the number of paths, $\alpha^{(i)}$ denotes the gain of the i-

th path, $\phi^{(i)}$and $\theta^{(i)}$ represent the azimuth and elevation AoAs of the incident plane wave, respectively; and $A(\phi^{(i)}, \theta^{(i)})$ refers to the antenna array response matrix, which is determined by its geometry.

2.3 Array Configuration

For a typical ULA with n antennas, we have [19]

$$a_{ULA}(\xi) = \frac{1}{\sqrt{N}}[e^{-j2\pi\xi n}]_{n\epsilon q(N)} \quad (2)$$

where, $q(N) = \{n - (N-l)/2, \quad n = 0,,1,2,\dots,N-1\}$. The spatial directions are given by $\xi = \frac{d\sin\theta}{\lambda}$ for ULAs, where θ , λ and d, represent the physical direction, wavelength of carrier, and antenna spacing respectively, which commonly meets d = λ / 2 in mm-wave communications.

The Eq. (1) has been reported in terms of MN because it considers the total number of communication links between the M Rx and N Tx antennas, leading to MN possible signal paths, not just the individual antennas. The array's response can be described as the cumulative effect of these signal paths on the overall communication system, showcasing the combined influence of the Rx and Tx antennas, as written in (3).

$$a_{ULA}(\xi^{azi}, \xi^{ele}) = \frac{1}{\sqrt{N}}\left[e^{-j2\pi\xi m}\right] * [e^{-j2\pi\xi n}] \quad (3)$$

$m = [0,1,\dots,M-1]^T$, $n = [0,1,\dots,N-1]^T$, the azimuth and elevation angles can be described as $\xi^{azi} \triangleq d\sin(\theta_{azi})\sin(\theta_{ele})/\lambda$ $\xi^{ele} \triangleq d\cos\theta_{ele}/\lambda$, are the spatial angles.

2.4 Antenna Design

The antenna dimension for the system was calculated using [20] with some modifications to make the antenna as compact as possible since the dimensions were designed for 100 antenna elements, but in this design, 64 antenna elements are used for the antenna array system.

The resonant frequency selected for the design was 28 GHz. A planar antenna array configuration was used for the transmitter and receiver, with Yr and Zr antennas on the horizontal and vertical axes for the receiver and Yt and Zt antennas for the transmitter. At frequencies of 28 GHz in the millimeter-wave range, the reduced wavelength results in very compact antenna arrays, leading to the assumption that all the antennas within the array experience the similar scattering environment. This compactness means that all antennas are in close proximity to each other relative to the wavelength, simplifying the analysis process by enabling uniform handling of the received signals throughout the array [21].

Since the frequency used in this research is 28 GHz, the wavelength (λ) is 1.07 mm, and the antenna element spacing (d) is 0.53 mm. After designing the parameters, 64 antenna elements are arranged in an array with inter-element spacing of λ/2 in a planar configuration, with $\varepsilon_r = 2.2$.

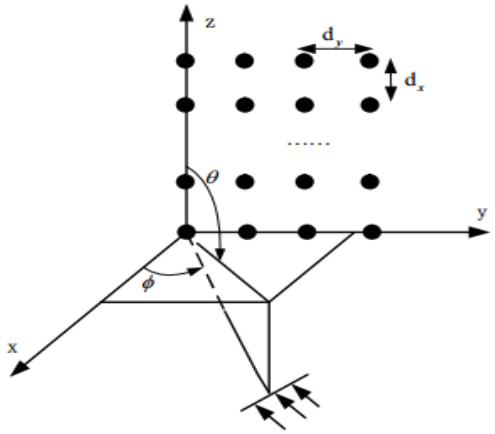

Fig. 4 An illustration of the UPAs.

In Fig. 4, which shows an illustration of the UPAs that the BS consists of Nt(h) and Nt(v) transmit antenna elements in horizontal and vertical directions, respectively, the corresponding to inter-antenna spacing is denoted as dy and dx, θ and φ denote the elevation and azimuth angles of AODs.

2.5 Beamspace Creation

In accordance with the depiction in Fig. 4, the process of beamspace formation is accomplished by employing a meticulously engineered electromagnetic lens, which is responsible for concentrating electromagnetic energy. This results in the conversion of scattered millimeter waves into focused directional beams. The transition from the spatial domain to the beamspace domain streamlines various processing operations, such as beamforming and channel estimation, enhancing the effectiveness of communication. Within the beamspace domain, signals are depicted as directional beams rather than their original spatial sources, thereby further streamlining processing tasks.

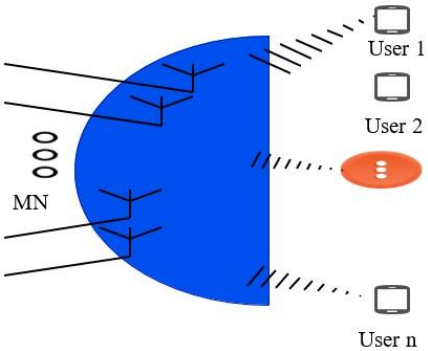

Fig. 5 Massive MIMO lens antenna array operating at millimeter waves.

The antenna array of lens type signified by matrix (U), which has M guiding vector beams that are orthogonal across a full-angle space, performs the Fourier transform in a discrete domain of space [22].

$$U = [a(\Psi_1), a(\Psi_1), \dots, a(\Psi_N)]^H \quad (4)$$

where,

$$a(\Psi) = \frac{1}{\sqrt{N}}[e^{-j2\pi\Psi m}]_{m\in I_N} \quad (5)$$

$$I_N = \left\{p - \frac{(N-1)}{2},\ p = 0, \dots, N-1\right\} \quad (6)$$

$$\Psi = \frac{d}{\lambda}\sin\theta,\ d = \frac{\lambda}{2}$$

$$\Psi_N = \frac{1}{N}\left(n - \frac{N+1}{2}\right),\ \text{n=1, 2… N} \quad (7)$$

where, U- Spatial discrete fourier transform (DFT) matrix, $a(\Psi)$- is $N \times 1$ array steering vector, N- Number of beams, Ψ_N- Antenna arrays of lens type in order to pre-define spatial directions, θ -is the physical direction, λ -is the wavelength of carrier, and d -is the antenna spacing which usually satisfies d = λ/2

As explained in [23], mm Wave massive MIMO with an antenna array of lens type may substantially decrease the quantity of needed RF chains without evident performance loss because of the beamspace channel's $\widehat{H}$ sparse nature.

This lens antenna array acts as a passive phase shifter to culminate the sparse beams; thus, using successful beam estimation algorithms will give us good efficiency, while using active phase shifter networks leads to more cost and energy consumption than lenses.

2.6 Beamspace Channel Model

Beamspace MIMO can be calculated by multiplying the traditional MIMO by using the spatial DFT matrix U[22].

Given the channel model in Eq. (1), the antenna array of the lens type system model for millimeter waves can be explained using the mathematical model as follows using [22].

$$\tilde{y}^{DL} = H^H U^H P_s S + n \quad (8)$$

In the antenna array of lens type, the whole space is covered by the array guiding vectors of N perpendicular orientation, which are contained in a spatial DFT matrix that is U of dimensions $N \times N$ written as.

$$U^H = [a(\Psi_1), a(\Psi_1), \dots, a(\Psi_N)]^H$$

Now we can define the beamspace channel by multiplying the traditional MIMO by the spatial DFT matrix.

$$\widehat{H} = HU = [\tilde{h}_1, \tilde{h}_2, \dots, \tilde{h}_k] = [Uh_1, Uh_2, \dots, Uh_k,]$$

$$\widehat{H} = \sqrt{\frac{MN}{P+1}}\sum_{i=0}^{P}\alpha^{(i)}A(\xi^{azi^{(i)}}, \xi^{ele^{(i)}}) * [a(\Psi_1), a(\Psi_1), \dots, a(\Psi_N)]^H + n \quad (9)$$

The vector of the channel in beamspace connecting the BS and the user K is denoted by $\tilde{h}_k$. Because of the restricted number of dominating scatterers in the mm-Wave prorogation environments [24], [25], [26], [27], the beamspace channel $\widehat{H}(\tilde{h}_k)$ exhibits a sparse structure [28]. As a result, based on the sparse beamspace channel, we can select only a small number of acceptable beams to lower the size of the MIMO system as

$$\tilde{y}^{DL} = \tilde{H}_r{}^H P_{rS} S + n \quad (10)$$

where $\tilde{H}_r = \tilde{H}(b,:)_{b\epsilon \mathrm{B}}$with B stands for the sparsity mask, which is the beam set that comprises the selected beam indices [29], and the associated dimension-reduced matrix of the digital precoder designated as Pr.

All the hardware components required for Switch phase shifter lens (SPL) implementation are N switches, N^2M 1-bit phase shifters, and RF Lens.

The analog RF precoding matrix can be explained as

$$F_{RF} = SP_s U^H \quad (11)$$

where the switch matrix has the dimension of $N_{P_s} \times N_s$, while having the RF and baseband precoders and combiners, an effective matrix is created which can be shown using the model as follows.

$$\widehat{H} = W_{BB,k}^H W_{RF,k}^H H F_{RF} F_{BB} \quad (12)$$

Beam selection requires information from beamspace channel$\widehat{H}$. to achieve capacity-approaching performance. The estimated beamspace channel will not experience a major SNR loss in large MIMO-based mm-wave antenna arrays of lens type because beamforming improvements are always present in these systems [21]. However, anticipating the channel of beamspace with minimal pilot overhead is still a challenge because of the limited RF chains and the large region of the beamspace channel.

2.7 Beamspace Channel Estimation

First, a pilot transmission strategy was performed. Then, for channel estimation, an adaptive choice network was built to acquire the most efficient measurements of the beamspace channel. To estimate the channel of beamspace using reduced pilot overhead and performance, which is reliable, a support detection (SD) and orthogonal matching pursuit (OMP)-based channel estimation scheme was utilized. Finally, a performance assessment was demonstrated to show the benefits of the proposed method.

Considering a transmission strategy in which there are n blocks made up of K instants each, separated into Q instants, where $Q = nK$, given a pilot matrix of size $K \times K$, which consists of K users transmitting a mutually perpendicular pilot sequence within K instants. At the base station (BS) in the nth block, the received uplink signal matrix with dimensions N × K can be shown as $\tilde{Y}_n^{UL} = \widehat{H}\psi_n + N_m$, where N_m is NM× K noise matrix and $n = 1,2, \dots, NM$.

2.8 Proposed Adaptive Selecting Network

For N_t antennas and K_t RF transmit chains, N_s data streams are required to send to the receiver. The transit beamforming matrix F_{BB} is of size $K_t \times N_s$ and matrix of RF precoder dimension $N_t \times K_t$. F_{RF} is employed through RF switches or analog phase shifters. Then the precoder matrix can be given by$F_{RF} = F_{RF}F_{BB}$. Similar to the transmitter, the $K_r \times N_s$ matrix of the baseband beamformer W_{BB} and the $N_r \times K_r$ RF matrix of the combiner W_{RF} make up the receive beamformer $W = W_{RF}W_{BB}$ [22], [30].

$$\tilde{y}^{DL} = \widetilde{H}_r{}^H W_{BB}^H W_{RF}^H F_{RF} F_{BB} + W_{BB}^H W_{RF}^H n \quad (13)$$

Multiplying the downlink receive vector by an RF lens will give us RF lens embedded switch or phase shifter Network$\widehat{H}$=$HU = [\tilde{h}_1, \tilde{h}_2, \dots, \tilde{h}_k] = [Uh_1, Uh_2, \dots, Uh_k,]$

$$\tilde{y}^{DL} = W_{BB}^H W_{RF}^H \widehat{H}_r{}^H F_{RF} F_{BB} + W_{BB}^H W_{RF}^H n \quad (14)$$

For a switch phase shifter network changing the precoding and combiner metrics. The transit beamforming matrix F_{BB} is of size $K_t \times N_s$ and matrix of RF precoder with dimension $N_t \times K_t \times N_s$, the beamformer of receiver $W = W_{RF}W_{BB}$ is made of the $N_r \times K_r$ RF combining matrix W_{RF} and $N_r \times N_r \times K_r$ is matrix of baseband beamformer W_{BB}. The same replacement can be made for embedding RF-Lens antenna array. The mathematical details for the analog and baseband precoder matrices can be shown here

- $F_{RF} = N_t \times K_t$ for analog phase shifters or RF switches
- $F_{RF} = U \times N_t \times K_t$ for Lens embedded analog phase shifters or RF switches
- $F_{RF} = N_t \times N_{ps} \times K_t$ for Phase shifter and RF switch
- $F_{RF} = U \times N_t \times N_{ps} \times K_t$ for Lens embedded Phase shifter and RF switch
- F_{BB}= $K_t \times N_s$ for all the networks

Based on the above equations of F_{RF} and F_{BB} the dimension for all the structures can be inserted in to the equation for the downlink vector. Also detail matrix manipulated can be shown in the calculation in the complexity analysis.

Employing a combiner W_m of dimension NM × K to combine the uplink signal matrix of the receiver side, we can get R_n of dimension $K \times K$ in the baseband, and sampled by $N_{RF} = K$ RF chains as [22].

$$R_n = W_n \tilde{Y}_n^{UL} = W_n \widehat{H} \psi_n + W_n N_m \quad (15)$$

Next, the matrix of K × K measurement $Z_m$of the channel of beamspace $\widehat{H}$can be constructed through multiplication of the familiar pilot matrix ψ_n^Hon the right side by

$$Z_m = R_m \psi_n^H = W_n \widehat{H} + N_m{}^{eff} \quad (16)$$

As previously indicated, in order to ensure that the measurement vector $\overline{\mathrm{Z}}_{\mathrm{k}} = W_n \tilde{h}_k + n_{n,k}{}^{eff}$ contains all of the information related to the beamspace channel $\tilde{h}_k$, it is necessary for the number of pilot symbols Q to be at least greater than n. This requirement is still high for mm-wave massive MIMO systems [22]. Thus, it proposes adaptive selecting network replacing the conventional Switch network with a 1-bit phase shifter thus it guarantees $\overline{\mathrm{Z}}_{\mathrm{k}}$ has the complete information of $\tilde{h}_k$ even if $Q < n$. Such a formulation's motive can greatly lower the quantity of pilot symbols, but at the expense of considerable SNR loss.

Now the goal is designing the analog combiner W_n or $\overline{w}$ with the lowest achievable mutual coherence

$$\mu \triangleq \max_{i \neq j} \left| \overline{w}_i^H \overline{w}_j \right| \quad (17)$$

where $\overline{w}_i$ is the i[th] column. Certain matrices have previously been demonstrated to benefit from small μ, such as the i.i.d. Gaussian random matrix [31]. Assuming an uplink noise vector $\overline{n}_k$ Z follows the distribution $\mathrm{CN}(0, \sigma_{UL}^2 I)$ and define $\delta \triangleq \sqrt{2\sigma_{UL}^2(1+\alpha)\ln n}$ where $\alpha > 0$ is a constant. Then, we have probability

$$pr\left\{ \max_{1 \leq n \leq NM} \left| \overline{w}_n^H \overline{n}_k \right| < \delta \right\} \geq \left(1 - \frac{1}{N^{\alpha}\sqrt{\pi(1+\alpha \ln n)}} \right)^{NM} \quad (18)$$

where $\overline{w}_n$ is the nth column of the combiner $\overline{w}$.

2.8.1. Orthogonal Matching Pursuit and Support Detection Based Beamspace Estimation

In order to produce the beamspace domain channel, the traditional compressive sensing algorithm, such as the orthogonal matching pursuit (OMP) method, employs a larger digital precoder followed by a large number of RF chains. But when the SNR is low, the user transmits with less power, which results in less beamforming gain. As a result, the data in $\check{h}_k$is more vulnerable to noise. On the other hand, precision is sacrificed in order to lower channel overhead when support detection is used instead of the OMP algorithm. Therefore, after determining the effective combiner network and creating the beamspace channel, an analog combiner with reduced mutual coherence is utilized to increase accuracy [22].

2.9 Performance Measurement Metric

After finding the effective channel matrix using the channel estimators with the zero forcing (ZF) precoding, the achievable sum-rate for a full system is given as [32].

$$R = K \log(1 + \frac{\gamma}{Ktr[(\widehat{H}^H \widehat{H})]^{-1}}) \quad (19)$$

where, H-is the channel matrix, K-is the number of users.

The spectrum efficiency could be computed from the achievable sum rate using (21). The achievable spectral efficiency is obtained by normalizing the rate with respect to the signaling interval and available bandwidth.

$$SE = \frac{R}{(W * T_{symbol})} \quad (20)$$

where, $T_{symbol} = \frac{(1+R^*)}{W}$, $R^*$is the roll off factor performance, w- Bandwidth of system, T_Symbol-Symbol time.

Finally, the energy efficiency can be found by dividing the achievable sum rate by the total power consumed by all elements. Which can be given by.

$$\zeta = \frac{R}{P+P^*+N_{RF}P_{RF}} \quad (21)$$

where, $P = P_{ps} = 30mW$ is the phase shifter's power consumption, $P^* = P_{ps} = 5mW$ is the switch's power consumption, $P_{RF} = 250\,mW$ is the power consumed per RF chain

2.9.1. Capacity of System

The maximum rate at which data may be sent over a channel is known as the channel capacity, or C. It is possible to assess each RF chain's capacity in the mm-wave system [33].

$$C = B * \log(det(I_k + \frac{\gamma}{N_{eff}} \widehat{H}^H \widehat{H})) \quad (22)$$

where, C=capacity of system in bit/s, B=bandwidth of the system, I_k= identity matrix, γ=SNR values, N_{eff}=total number of RF chains, H=channel matrix

2.9.2. Complexity Analysis

Addressing the computational cost in beamforming networks involves utilizing the sesquilinear matrix form to streamline complexity calculations. By breaking down the effective channel matrix into simpler computational steps, the matrix-vector multiplication and summation processes become more manageable. The total computational complexity varies with the configuration of phase shifters and switch networks, depending on the number of RF chains or users supported. This structured approach allows for an efficient calculation of the overall complexity, balancing the trade-offs between performance and computational load. Specifically, the effective channel matrix, given as $\widehat{H} = W_{RF,k}^H H F_{RF}$, can be described in a sesquilinear form to simplify these calculations.

Sesquilinear Form $C^H Ab$

The Sesquilinear form $C^H Ab$ should be evaluated by computing the matrix-vector product Ab in a first step and then multiplying with the row vector C^H from the left-hand side. The matrix vector product requires MN multiplications and $M(N-1)$ summations, whereas the inner product needs M multiplications and $M-1$ summations. Altogether, $M(N+1)$ multiplications and $MN-1$ summation have to be computed for the Sesquilinear form $C^H Ab$, yielding a total number of $2MN + M - 1$ flops.

Phase shifter or Switch

From Eq. (13), we have the effective channel matrix which is given by $\widehat{H} = W_{RF,k}^H H F_{RF}$ by using two stage precoding technique, where the matrix dimensions are

$W_{RF} = N_r \times K,\ H^H = N_r \times N_t, W_{RF} = N_t \times K$

$$\widehat{H} = N_r \times K * (N_r \times N_t \times N_t \times K) = 1 \times N_r \times (N_r \times N_t \times N_t \times 1) * K^2 \quad (23)$$

where $(N_r \times N_t \times N_t \times 1)$ require $N_r * N_t$ multiplications and the $1 \times N_r \times (N_r \times 1)$ requires N_r multiplications. Thus, for the phase shifter configuration.

$\widehat{H} = K^2 N_r (N_t + 1)$

But for the switch network the difference comes in the number of RF chains or the number of users supported by the (K=4 and $N_{RF} = 4$) in this case.

$\widehat{H} = K^2 N_r (N_t + 1)$

The total complexity can be found by incorporating the baseband precoder on the existing hybrid precoder which can be given by

$$Complexity_{Total} = K^2 N_r (N_t + 1) + \frac{3K^3}{2} + \frac{K^2}{2} \quad (24)$$

Phase shifter and Switch

The complexity of the equation for the phase shifter and switch was calculated, and then the total complexity from the side of the transmitter was computed.

$SW = \frac{N_t}{2} \times K$ and $PS = N_t \times K$

For the switch network $\widehat{H} = K \times N_r \times (N_r \times N_t \times \frac{N_t}{2} \times K)$ require $\frac{N_r * N_t}{2}$ multiplication and the $1 \times \frac{N_r}{2} \times (N_r \times 1)$ requires $\frac{N_r}{2}$ multiplications. Which gives a complexity of $\frac{K^2 N_r}{2}(N_t + 1)$. Thus, adding the phase shifter complexity will yield a total complexity for the phase shifter and switch network

$\widehat{H} = \frac{K^2 N_r}{2}(N_t + 1) + K^2 N_r (N_t + 1)$, $\widehat{H} = \frac{3K^2 N_r}{2}(N_t + 1)$

Finally, total complexity with the baseband precoder can be shown as.

$$Complexity_{Total} = \frac{3K^2 N_r}{2}(N_t + 1) + \frac{3K^3}{2} + \frac{K^2}{2} \quad (25)$$

3 Results and Discussion

Using the equations in Section 2, the spectral efficiency of a lens-embedded planar antenna array for mm-wave massive MIMO has been analyzed. The plot for the spectral efficiency represents the system that uses a Saleh Valenzuela channel model, OMP and SD-based channel estimations, and a lens antenna system to create the beamspace channel. The work discusses the spectral efficiency without lens antenna networks to clearly show the advantages of putting RF lenses on our traditional MIMO system. Throughout this paper, traditional MIMO describes mm-wave MIMO channels without lens antenna array networks. The achievable sum rate, followed by the spectral efficiency, is analyzed for both

the traditional and beamspace MIMO configurations. The advantages of beamspace MIMO have been clearly shown using the simulation using the previously defined mathematical models.

Table 1 Input parameters and values

Parameters	Input
Number of users	K
Antenna	MN Lens antenna array
Connections	Fully connected (N^2M) phase shifters
Phase shifter	1-bit PS
Channel Model	Saleh Valenzuela
Channel Estimation	OMP and SD-based
RF-chain	Equal to number of users(K)
Beamforming	ZF

3.1 Spectral Efficiency

Studying the spectral efficiency of ZF precoding in multiuser large multiple-input multiple-output systems. The following setups have been compared using channel estimations based on both OMP and SD. The following configurations are employed in performance analysis:

- Switch, Lens
- 1-bit phase shifter, Lens
- Switch only
- 1-bit phase shifter only
- Switch, 1-bit phase shifter
- Proposed switch, 1-bit phase shifter, Lens

It is important to remember that each one uses a uniform planar array arrangement, which is derived from the mathematical model that is discussed in Section 2.

As described in Figs. 6 and 7, six different arrays have been shown, including the proposed system, which is a combination of a switch, phase shifter, and lens antenna array. The proposed system shows better performance at lower SNR levels, while the others show decreased overall performance. As shown in the Figs., the UPA-based switch phase shifter network performs the least, mainly due to the absence of a lens and the lower resolution of the phase shifters, which shows us that using phase shifters and switches without RF lenses will not give us good performance due to the poor resolution of 1-bit PSs while used along the UPA structures.

This can work for both the SD and OMP-based channel estimates, but the OMP-based estimation experiences reduced performance. Employing 2-bit phase shifters instead of 1-bit variants could facilitate more precise phase control, thereby enhancing the accuracy of beamforming and mitigating interference within the proposed network. However, this increased precision comes with added complexity in terms of hardware and signal processing. Such enhancements have the potential to increase spectral and energy efficiency, making the network more capable of accommodating numerous users with a reduced number of RF chains.

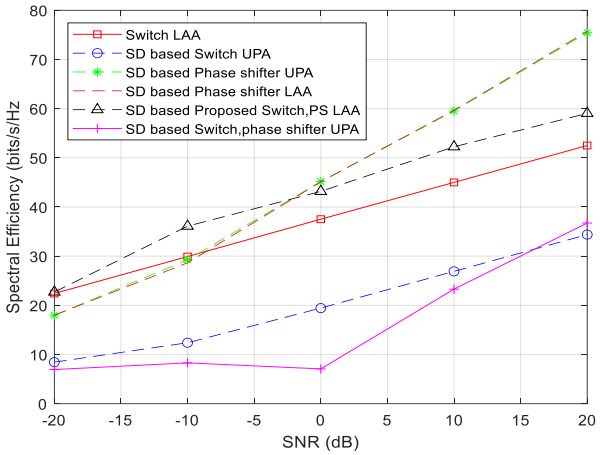

Fig. 6 Spectral efficiency of SD-based channel estimation using K=N_RF=4 and MN=64 antennas using ZF precoding technique.

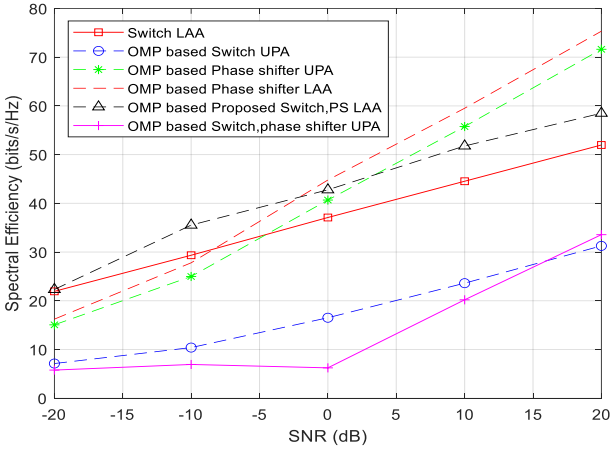

Fig. 7 Spectral efficiency of OMP-based channel estimation using K=N_RF=4 and MN=64 antennas using ZF precoding technique.

Different values have been shown for different SNR levels; a maximum SE of 71.62 bit/s/Hz is observed using SD-based channel estimation, from which a 40 bit/s/Hz increase is observed from that of the Switch-UPA structure at the 20-dB level.

3.2 Energy Efficiency

Once the achievable sum rate has been determined, the energy efficiency may be calculated by dividing the sum rate by the total energy used, taking into account the number of phase shifters, switches, and users, and multiplying each value by the respective number of that component.

The results can be shown in Fig. 8, which is based on the mathematical models drawn in Section 2. From the

values in Fig. 8, one can understand that the proposed structure has better energy efficiency compared to others. Its performance is close to that of the Switch LAA network in SD-based channel estimation, while the Phase Shifter LAA and Switch, Phase Shifter UPA, have the least efficiency because of the high number of phase shifters and switching networks. The same conclusion can be drawn as the result in Fig. 9, but with a decreased overall performance, which shows both spectral and energy efficiencies, the SD-based channel estimation outperforms our proposed model. Other performance measurements can be shown with the change of number of users and RF chains in parallel while keeping the number of antennas unchanged, which can be shown in Fig. 10 for both SD and OMP-based channel estimations.

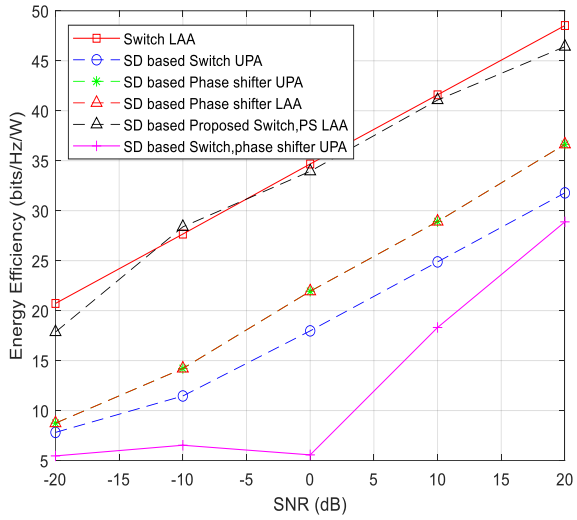

Fig. 8 Energy efficiency of SD- based channel estimation using K=N_RF=4 and MN=64 antennas using ZF precoding technique.

Fig. 10 shows an increase in spectral efficiency by increasing the number of users in parallel with an increase in the RF chains and a difference in spectral efficiency between the different networks based on ZF hybrid beamforming techniques while utilizing SD-based channel estimation. Fig. 10. shows that the proposed network shows better spectrum efficiency, while the UPA-based switch phase shifter network performs the least. The problem here is that due to the absence of the Lens antenna array network and the resolution of the l-bit phase shifter network, the switching mechanism between the phase shifter and the RF chain did not work properly, which leads to reduced spectral efficiency performance. As the number of RF chains increases in parallel with the number of users, the beamforming scheme goes to a ZF-based fully digital beamformer. Given a fully connected 1-bit PS network, N number of RF chains are connected, but as we can see from Fig. 10, we cannot increase the number of users indefinitely as we reach some point (41 users for 64 antenna elements in this case), and the spectrum efficiency shows a declining performance. The same conclusion can be drawn for the other configurations, but the main point here is finding the saturation point. What's interesting about the switch, phase shifter, and uniform planar array configurations is that as the number of users and RF chains in parallel grows, dashed lines appear at various points in the plot, indicating the number of RF chains that can support users without affecting spectral efficiency.

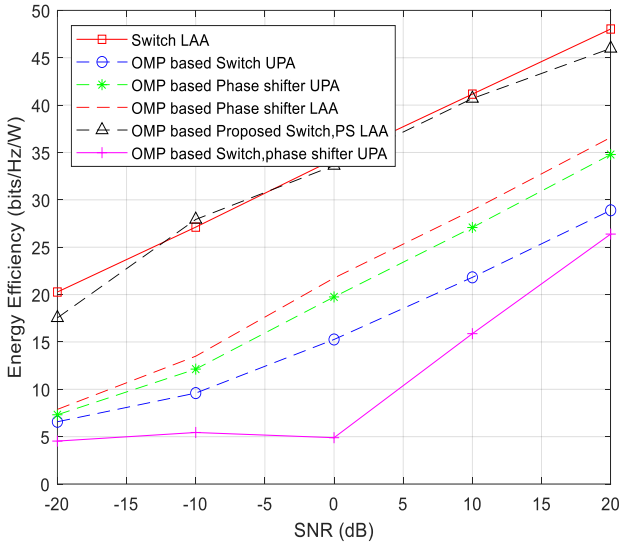

Fig. 9 Energy efficiency of OMP- based channel estimation using K=N_RF=4 and MN=64 antennas using ZF precoding technique.

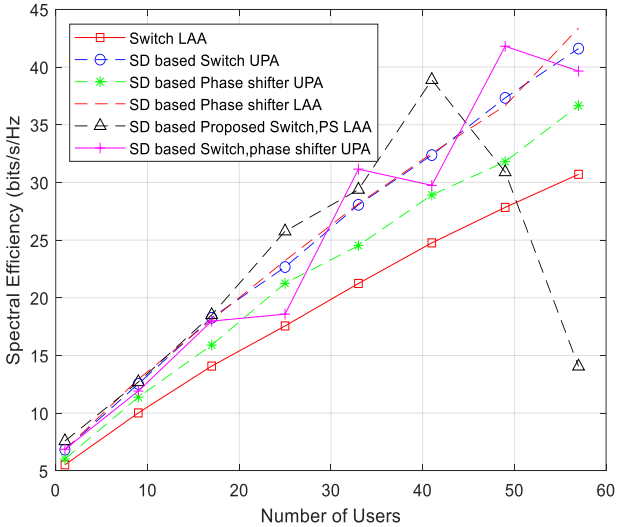

Fig. 10 Spectral efficiency of SD- based channel estimation using for increasing Number of users and MN=64 antennas for a using ZF precoding technique.

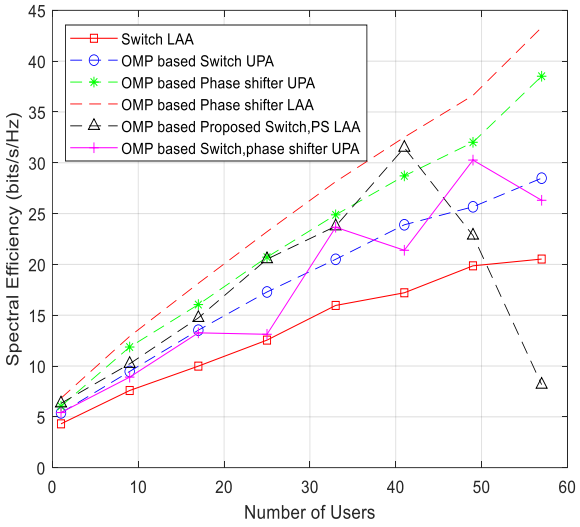

Fig. 11 Spectral efficiency of OMP- based channel estimation for increasing Number of users and MN=64 antennas using ZF precoding technique.

Fig. 11. is generated for the OMP-based LAA and UPA hybrid beamforming while the number of users and RF chains grow in parallel. For a fixed SNR value of 0 dB, this simulation has been done. The same results may be inferred from the description of the SD-based channel estimator, but the OMP-based channel estimator exhibits good but reduced performance, as stated throughout this work. Finally, we can infer that the proposed system and SD-based channel estimates operate well for a growing number of users approaching the saturation threshold indicated in Fig. 13.

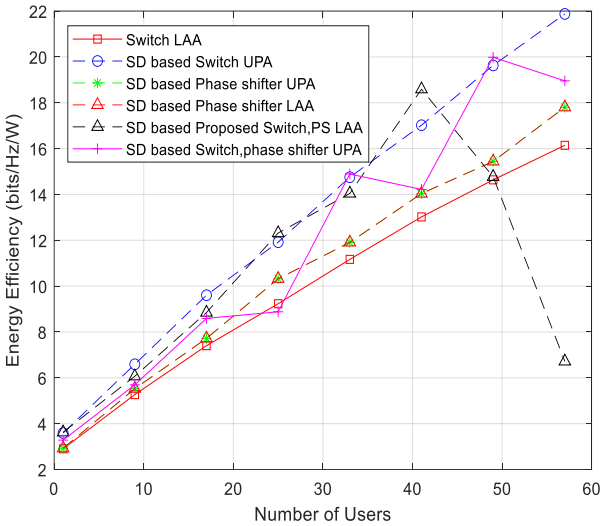

Fig. 12 Energy efficiency of SD- based channel estimation using for increasing Number of users and MN=64 antennas for an using ZF precoding technique.

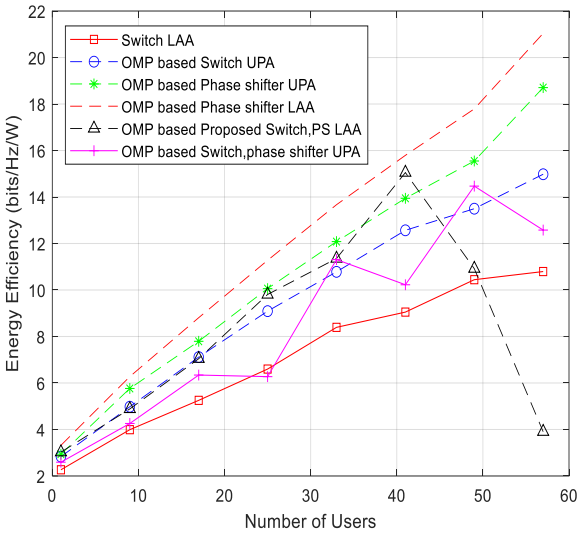

Fig. 13 Energy efficiency of SD- based channel estimation using for increasing Number of users and MN=64 antennas for an using ZF precoding technique

3.3 Capacity of the System

Overall system capacity is plotted using the mathematical Eq. (18). using the proposed model and both channel estimation techniques as shown in Fig. 14. which clearly indicates using the SD based channel estimation gives better system capacity which shows overall increased performance.

For a bandwidth of 1 GHz, the plot in Fig. 14 has been shown, which indicates the system capacity as we increase with SNR from low to high, which shows a slight increase in capacity. As shown in the Fig. 14, it achieves a maximum capacity of 18.39 Gbps at 20 dB.

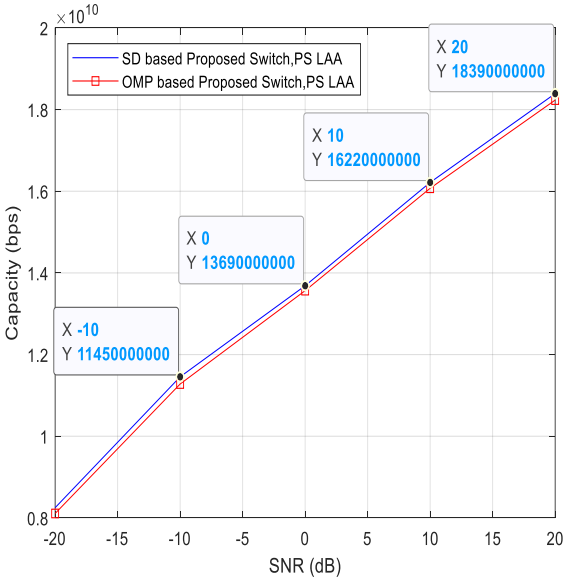

Fig. 14 Capacity of a single RF chain using the two channel estimation techniques for a total of K RF chain and users.

3.4 Computational Complexity

Fig. 15 depicts a plot for three configurations based on the equation of total complexity from Section 2. The phase shifter, switch, and phase shifter switch computations have been tested with and without a lens antenna array. To calculate the total complexity, the total number of multiplications and divisions was counted.

As shown in the Fig. 15, there is a clear set of differences between the computational complexities, with the SPS (switch phase sifter) network having the highest computational complexity. This is due to the addition of switches between the PS and RF chains, which will result in increased complexity over PS-only networks. When compared to a phase shifter-only network, the switch-only network has the lowest complexity due to the lower number of switches. We can see that including a lens antenna does not change the computational difficulty because multiplication by a scalar or by an array steering vector does not change the total degree of complexity. Finally, what we can note here is that the proposed system achieves optimum performance at the expense of higher computational complexity.

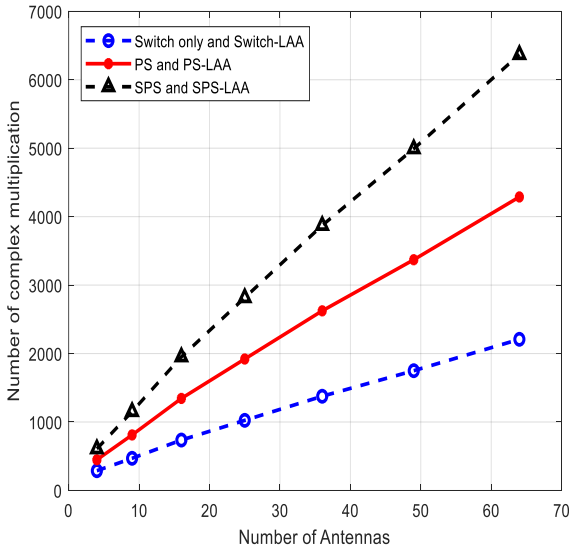

Fig. 15 Computational complexity.

4 Conclusion

This work demonstrated the spectral and energy efficiency of a hybrid switch, phase shifter, and lens network for hybrid beamforming over mm-wave massive MIMO and was compared with the other five configurations. The design makes use of the Saleh Valenzuela channel model, SD and OMP-based channel estimates, and ZF hybrid beamforming to create a uniform planar array arrangement with RF lenses. Using the SD-based channel estimator due to the best performance for the proposed system and taking 20 dB point as a sample SNR value, the phase shifter UPA and phase shifter LAA achieve a SE of 75.1 bps/Hz while the switch, PS, UPA achieves 36.74 bps/Hz, which shows a slight improvement from switch-UPA networks, but the proposed switch, PS, LAA gives a moderate performance of 59.04 bps/Hz, which increases by 6.9 bps/Hz from that of Switch LAA network, where the EE metric shows good performance next to switch LAA network outperforming all configurations. It was also demonstrated that the suggested network can transmit up to 18.39 Gbit/s at 20 dB over a bandwidth of 1 GHz, achieving optimum performance at the cost of higher computational complexity. The future work of this research will include other non-linear beamforming techniques that are adaptable to the network, or even other linear precoding approaches that could be considered for increased efficiency. This work can be further extended by using a well-designed electromagnetic lens and a high-resolution phase shifter to increase the efficiency of the system.

Conflict of Interest

The authors declare no conflict of interest.

Author Contributions

Conceptualization, methodology, software, validation, and investigation: Tadele. A. Abose, Thomas O. Olwal, Abel D. Daniel, and Murad R. Hassen; draft preparation: Tadele. A. Abose, Abel D. Daniel, and Murad R. Hassen; editing: Tadele. A. Abose, and Thomas O. Olwal. All authors have read and agreed to the published version of the manuscript.

Funding

This research did not receive any specific funding.

References

[1] S. Ashraf, J. A. Sheikh, A. Ashraf, and U. Rasool, "5G Millimeter Wave Technology: An Overview," *Intelligent Signal Processing and RF Energy Harvesting for State of art 5G and B5G Networks*, pp. 97-112, 2024.

[2] T. S. Rappaport, M. K. Samimi, and S. Sun, "Wideband millimeter-wave propagation measurements and channel models for future wireless communication system design," *IEEE Trans. Commun*, Vol. 63, No. 9, pp. 3029–3056, Sept. 2015.

[3] T. S. Rappaport, "Millimeter wave mobile communications for 5G cellular: It will work," *IEEE Access*, Vol. 1, pp. 335–349, May 2013.

[4] Jayakumar, Roscia JS, and Allwyn Clarence Asis Arul, "A Survey on Beamspace Millimeter-wave

Massive Mimo Systems: An Overview of Open Issues, Challenges, and Future Research Trends," *International Journal of Sensors Wireless Communications and Control*, Vol.14, No.1, pp.1-20, 2024.

[5] S. Hamid, S. R. Chopra, A. Gupta, S.Tanwar, B. C. Florea, D. D.Taralunga, and A. M. Shehata, "Hybrid Beamforming in Massive MIMO for Next-Generation Communication Technology," *Sensors*, Vol. 23, No.16, 2023.

[6] J. Lv, T. Wang, and S.Wang, "Optimal analog precoder design for hybrid beamforming is possible," *IEEE Transactions on Vehicular Technology*, 2023.

[7] A. Alkhateeb, J. Mo, N. Gonzalez-Prelcic, and R. W. Heath, "MIMO precoding and combining solutions for millimeterwave systems," *IEEE Commun. Mag.*, Vol. 52, No. 12, pp. 186 – 195, Feb. 2014.

[8] J. Li, L. Zhao, and Y. Jiang, "Hybrid Analog and Digital Precoding Design for Minimum BER in Massive MIMO System," *IEEE Transactions on Vehicular Technology*, 2024.

[9] S. Biru, S. Mishra, R. S. Singh, S. Chura, and S. Satapathy, "Energy-efficient hybrid beamforming for millimeter-wave-based massive multiple-input multiple-output system," *International Journal of Communication Systems*, Vol. 37, No. 8, 2024.

[10] K. Umaria, and S. Shah, "Spectral efficiency of hybrid precoding and combining design for mm-Wave multi-user massive MIMO systems," *Analog Integrated Circuits and Signal Processing*, pp.1-9, 2024.

[11] X. Qi, M. Peng, H. Zhang, and X. Kong, "Anti-Jamming Hybrid Beamforming design for Millimeter-Wave Massive MIMO systems," *IEEE Transactions on Wireless Communications*, 2024.

[12] Y. N. Samir, H. B. Nafea, and F. W. Zaki, "Performance Evaluation of Spectral Efficiency Hybrid Precoding and Combining Algorithm for Millimeter Wave-MIMO Systems," *Wireless Personal Communications*, Vol. 133, No. 3, pp. 1769-1784, 2024.

[13] R. A. Mohammad, Yassin, and H. Abdallah, "Hybrid Beamforming in Multiple User Massive Multiple Input Multiple Output 5G Communications System," *in 2020 7th International Conference on Electrical and Electronics Engineering (ICEEE)*, Antalya, Turkey, 2020.

[14] Nosrati, H., Aboutanios, E., Wang, X., & Smith, D., "Switch-based hybrid beamforming for massive MIMO communications in mmWave bands," *Signal Processing*, Vol. 200, 2022.

[15] Cetinkaya, S., Afeef, L., Mumcu, G., & Arslan, H, "Heuristic inspired precoding for millimeter-wave MIMO systems with lens antenna subarrays," *In 2022 IEEE 95th Vehicular Technology Conference:(VTC2022-Spring)*, Helsinki, Finland, 2022.

[16] Méndez-Rial, R., Rusu, C., González-Prelcic, N., Alkhateeb, A., & Heath, R. W., "Hybrid MIMO architectures for millimeter wave communications: Phase shifters or switches?" *IEEE access*, Vol. 4, pp. 247-267, 2016.

[17] Payami, S., Khalily, M., Loh, T. H., & Nikitopoulos, K., "Hybrid beamforming with switches and phase shifters over frequency-selective channels," *IEEE Wireless Communications Letters*, Vol. 9, No.8, pp. 1305-1308, 2020.

[18] Nosrati, H., Aboutanios, E., Wang, X., & Smith., "Switch-based hybrid beamforming for massive MIMO communications in mmWave bands," *Signal Processing*, Vol. 200, 2022.

[19] L. Zhao, J. Li, S. Huang, X. Wu, and M. Jiang, "Low-complexity hybrid precoding for sub-connected millimeter wave massive MIMO systems," Signal Processing, Vol. 219, 2024.

[20] T.Yuwono, M. Ismail, and I. Hajar, "Design of Massive MIMO for 5G 28 GHZ," *In 2019 2nd International Conference on Computer Applications & Information Security (ICCAIS)*, Riyadh, Saudi Arabia, 2019.

[21] M. Abdelfatah, A. Zekry, and S. ElSayed, "Orthogonal beamforming technique for massive MIMO systems," *Annals of Telecommunications*, pp. 1-19, 2024.

[22] X. Gao, L. Dai, S. Han, I. Chih-Lin, and X. Wang, "Reliable Beamspace Channel Estimation for Millimeter-Wave Massive MIMO Systems with Lens Antenna Array," *IEEE Transactions on Wireless Communications*, Vol. 16, No. 9, 2017.

[23] H. Song, and A. Sayeed, "Beamspace MIMO transceivers for low-complexity and near-optimal communication at mm-wave frequencies," *in 2013 IEEE International Conference on Acoustics, Speech and Signal Processing, Vancouver*, BC, Canada, Apr. 2013.

[24] A. Alkhateeb, G. Leus, and R. W. Heath, "Channel estimation and hybrid precoding for millimeter wave cellular systems," *IEEE J. Sel. Top. Signal Process.*, Vol. 8, No. 5, pp. 831–846, Oct. 2014.

[25] T. A. Abose, T. O. Olwal, and M. R. Hassen, "Hybrid beam-forming techniques for multi-cell massive MIMO," *International Journal of Advanced Technology and Engineering Exploration*, Vol. 9, No.94, 2022.

[26] T. A. Abose, T. O. Olwal, and M. R. Hassen, "Hybrid beamforming for millimeter wave massive MIMO under multicell multiuser environment," *Indian J Sci Technol*, Vol.15, No. 20, pp.1001-1011, 2022.

[27] T. A. Abose, T. O. Olwal, and M. R. Hassen, "Hybrid beamforming for millimeter wave massive MIMO under hardware impairments and imperfect channel state information," *in 2021 IEEE International Conference on Mobile Networks and Wireless Communications (ICMNWC)*, Tumkur, Karnataka, India, 2021.

[28] J. Brady, N. Behdad, and A. M. Sayeed, "Beamspace MIMO for millimeter-wave communications: System architecture, modeling, analysis, and measurements," *IEEE Trans. Antennas Propag.*, Vol. 61, No. 7, pp. 3814–3827, Jul. 2013.

[29] J. Hogan and A. Sayeed, "Beam selection for performance-complexity optimization in high-dimension MIMO systems," *in 2016 Annual Conference on Information Science and Systems (CISS)*, Princeton, NJ, USA, Mar. 2016.

[30] X. Yu, J. Zhang, and K. B. Letaief, "Hybrid Precoding in Millimeter Wave Systems: How Many Phase Shifters Are Needed?" *in 2017 IEEE Global Communications Conference (GLOBECOM 2017)*, Singapore, 2017.

[31] W. U. Bajwa, J. Haupt, A. M. Sayeed, and R. Nowak, "Compressed channel sensing: A new approach to estimating sparse multipath channels," *Proc. IEEE*, Vol. 98, No. 6, pp. 1058–1076, Jun. 2010.

[32] P. V. Amadori and C. Masouros, "Low RF-complexity millimeter-wave beamspace-MIMO systems by beam selection," *IEEE Trans. Commun.*,, Vol. 63, No. 6, pp. 2212–2223, 2015.

[33] Nguyen, N. T., and K. Lee, "Coverage and Cell-Edge SumRate Analysis of mmWave Massive MIMO Systems with ORP Schemes and MMSE Receivers," *IEEE Trans. Signal Process*, Vol. 66, No. 20, pp. 5349–5363, 2018.

Dr. Tadele A. Abose received BSC degrees from Hawassa University by Electrical Engineering in 2011 and MSC and PhD degrees from Addis Ababa University by Electrical Engineering (Communication Engineering Specialization) in 2014 and 2023 respectively. He is currently University lecturer in Mattu University, Ethiopia. His research interests are cognitive radio, massive MIMO, millimeter wave communication, backhaul networks, multicarrier modulation schemes and interference management techniques. He serves as a reviewer in a number of Elsevier/Springer/IEEE conferences and journals.

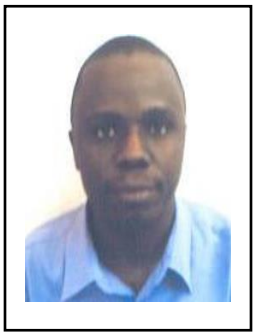

Thomas O. Olwal is a Senior member, IEEE. He received his Ph.D. degree in computer science from the University of Paris-EST, Champs-sur-Marne, France, in 2010, and the D.Tech. Degree in electrical engineering from Tshwane University of Technology (TUT) (in a cotutelle programme), Pretoria, South Africa, in 2011. He is currently lecturing at the TUT as a Professor and previously worked as Senior Researcher with Wireless Computing and Networking R&D, Council for Scientific and Industrial Research (CSIR). His research interests include analysis and design of the spectrum, energy-efficient radio resource management, Internet of Things, autonomous robotics, and automation and their emerging applications. He serves as a reviewer in a number of ACM/IEEE conferences and journals.

Abel D. Daniel received BSC and MSc degrees from Jimma and Dire Dawa University in Electrical Engineering in 2017 and 2022, respectively. His research interests are multicarrier modulation schemes, wireless communication, massive MIMO, and millimeter-wave communication.

Dr. Murad R. Hassen is a member, IEEE. He received his B.Sc, M.Sc and PhD in Electrical Engineering in 1993, 2001 and 2013, respectively from Addis Ababa Institute of Technology (AAiT), Addis Ababa University, Ethiopia. Currently he is working as Assistant Professor in the School of Electrical & Computer Engineering, AAiT. He has publications in International and national Journals. His research interests include development of highly efficient algorithms for smart antenna design and analysis, novel hybrid spectrum sharing for cognitive radio networks, and hybrid beamforming algorithms in millimeter wave massive MIMO.